GeoScience Engineering

INVESTIGATION OF FORCED-AIR DUCT LEAKAGE PHENOMENON USING CFD METHODS FOR UNDERGROUND TUNNEL CONSTRUCTION

Maciej KOSOWSKI[1], *Pavel ZAPLETAL*[1], *Grzegorz PACH*[2]
1 *VSB – Technical University of Ostrava, Faculty of Mining and Geology, Department of Mining Engineering and Safety, Ostrava, Czech Republic*
2 *Silesian University of Technology, Faculty of Mining, Safety Engineering and Industrial Automation, Gliwice, Poland*
E-mail: koso.pda@gmail.com

ABSTRACT

Using CFD, the paper deals with a simulation of all phenomena related to forced-air duct fitted with a fan, with the emphasis on unit aerodynamic resistance and untight air ducts. We created a 3-dimentional model of the system including perforations simulating untightens in order to make a computation network. Boundary conditions were set and calculations made in ANSYS Fluent 19.1 programme. The computational results were assessed using conventional methods used in mining operations and compared with the measurement results of real air ducts in mine workings. CFD is suitable to simulate forced-air ducts and allows for their more precise design.

Keywords: Auxiliary ventilation; CFD; Leaky forced-air duct; Tunnel construction.

1 INTRODUCTION

The article examines the potential of leaky forced-air duct modelling using CFD (Computational Fluid Dynamics) in the construction of tunnels. An auxiliary ventilation air duct consists of discrete mutually interconnected air ducts and fittings made of different materials. When combined with a fan, the operating point of the fan is bound with the air duct parameters. Due to the air duct length, diameter, type and quality, the air ducts have certain aerodynamic resistance, based on which a suitable fan is chosen to ensure sufficient air in the face. In the case of a leaky air duct, the situation is even more complex due to mass transport together with air exchange with ambient environment. The size of air loss due to leaky air ducts depends on a number of factors, particularly the tightness of the joints and air ducts [20], placement of fans in the duct, and the internal and ambient pressures.

Ventilation must be ensured during the construction of a tunnel. Due to the increase in tunnelling, civilian safety is becoming an important issue today [1]. However, the ventilation calculations get complicated due to air leaks occurring in the operated air ducts [2]. The implementation of auxiliary ventilation using a leaky air duct is based on the assumption of linear and constant leaks of air along the duct. The research in this article, thus, investigates whether it is possible to make a functional CFD model of a ventilation equipment manifesting all the phenomena related to auxiliary ventilation using a leaky forced-air duct, namely air leakage, total pressure drop, local resistance, linear resistance, and cooperation with the fan. If air duct modelling using computational fluid dynamics is successful, it shall permit further development and extension of models either by branching or placing auxiliary fans in the centre of the system. Such research will facilitate design of complex systems that cannot be precisely modelled at the moment based on analytical procedures [3]. CFD has been used to deal with mine ventilation problems and a number of authors have modelled the air duct using CFD. Researchers in [4] have compared the results of experimental measurements of air rates using an anemometer in the mine-working cross-section under the use of auxiliary ventilation. They also investigated the influence of the selected turbulence model on the agreement of CDF modelling results and the measured parameters. The research showed that Spallart-Allmaras

Vol. 68 (2022), No. 1
pp. 58–69, ISSN 1802-5420
DOI 10.35180/gse-2022-0069

turbulence model proved best for the purpose. The research, however, did not deal with air ducts and the air quantity at the outlet was set based on a fan theoretical operating point. The research did not incorporate duct untightens into the model. Researchers in [5] focused on the influence of location and size of air duct damage on the energy efficiency and fan operating point. They modelled one leak at a particular length of an air duct. It showed that the air quantity leaking due to the untightens falls to the second power of the distance from the fan. The relationship between the perforation size and the air leak is directly proportional and grows in a linear manner along with the width of the perforation. However, the untightens of the remaining air duct was not considered in the model. The study in [6] used CFD to prove the success and importance of auxiliary ventilation using air ducts at the crossing of longwall face and exhaust road. The authors compared the CFD modelling results and the experimental measurements of methane concentrations in the sites of CH4 sensors. The relative error was very low, which confirms the usefulness of CFD tools to deal with mine ventilation problems. Nevertheless, to simplify the computation, the air duct was modelled as an ideal tight duct. Based on measuring 20 air ducts in the operation of several black-coal mines, authors in [7,8] determined the values of real specific aerodynamic resistance and the mean coefficient of untightens, which we used to evaluate the CFD modelling results emerging from our research.

Although the above-mentioned authors have used CFD models of air ducts to deal with different mine working ventilation problems, there is no research available on the simulation of the air duct itself, or nobody has reported research examining the influence of untightens and resistance on fan cooperation. This research is valuable for tunnel constructors when more complex, branched air ducts need to be applied. The article is further structured as follows: Section 2 presents the CFD modelling method, while Section 3 describes and analyses the forced-air duct simulation using CFD, including the results.

2 MODELLING CFD

2.1 Model of turbulent flow k-epsilon and gas compressibility model

The flow is called turbulent if its variables show chaotic fluctuations in space and time. The major parameter to assess the flow rate turbulence intensity is the Reynolds number, being a dimensionless quantity related to force of inertia and viscosity (i.e. the medium resistance due to internal friction). It is used to determine whether the fluid flow is laminar or turbulent. The higher the Reynolds number, the lower the effect of friction forces of the fluid particles on the total resistance. To distinguish the laminar flow from turbulent (in duct flows), the Reynolds number for duct flow in the form below is used:

$$Re = \frac{\varrho \cdot \vartheta \cdot l}{\mu} \qquad (1)$$

where:

ϱ – density of fluid $\left[\frac{kg}{m^3}\right]$,
ϑ – fluid flow rate $\left[\frac{m^3}{s}\right]$,
l – duct diameter $[m]$
μ – fluid dynamic viscosity$[Pa \cdot s]$.

According to the results of CFD calculations, the flow rate at the fan inlet is 7.61 m^3/s, which renders the maximum air velocity at the air duct inlet of 9.69 m/s. The minimum air velocity at the air duct outlet is 6.18 m/s. The Reynolds numbers are calculated for both the cases:

$$Re_1 = \frac{1{,}25 \cdot 6{,}18 \cdot 1}{17{,}4 \cdot 10^{-6}} = 445\,965 \qquad (2)$$

$$Re_2 = \frac{1{,}25 \cdot 9{,}69 \cdot 1}{17{,}4 \cdot 10^{-6}} = 669\,199 \qquad (3)$$

In practice, for fluid dynamics inside a tube it is assumed that if Reynolds number is over 3000 [-], turbulent flow has developed fully [9]. This confirms the choice of the k – epsilon standard turbulence model as the right one. The two-equation statistical k - epsilon model determines the turbulent viscosity via two transport equations for k

Vol. 68 (2022), No. 1
pp. 58–69, ISSN 1802-5420
DOI 10.35180/gse-2022-0069

and ε. This model makes use of Boussinesq's hypothesis on the turbulent viscosity and related turbulent viscosity μ_t to k, ε and C_μ.

$$\mu_t = C_\mu \cdot \frac{k^2}{\varepsilon} \qquad (4)$$

where:

C_μ – empirical constant $[-]$,
ε – dissipation rate $[-]$,
μ_t – turbulent viscosity $\left[\frac{J \cdot s}{kg}\right]$,
k – turbulent kinetic energy $\left[\frac{J}{kg}\right]$.

The distribution of k is given by the transport equation. The extraction form of the transport equation for ϵ can be deduced from Naviers-Stokes equations as the transport equation contains complex dependences that need to be approximated. The k - epsilon model is suitable for high values of Reynolds numbers, ranging in the orders of Re=10^5 and higher. An important factor is the choice of gas compressibility model. The Ansys Fluent programme is equipped with two models, namely "*Incompressible Ideal Gas"* (in this form the density depends only on the working pressure and not on the field of local relative pressure) and "*Ideal Gas*" (which treats gas density on the basis of the total local pressure). To decide whether use a compressible or incompressible gas model, it is vital to calculate Mach number, which is one of the so-called characteristic numbers, i.e. a characteristic dimensionless physical quantity used in aerodynamics. It denotes the ratio of flow velocity through certain medium to the local speed of sound in the same medium. If Ma <0.1, the effect of medium compressibility is negligible [10]. It is calculated based on the following equation:

$$Ma = \frac{\vartheta}{c}, \qquad (5)$$

where:

ϑ – fluid flow rate $\left[\frac{m^3}{s}\right]$,
c – speed of sound in the fluid $\left[\frac{m}{s}\right]$.

In the model, we used operation barometric pressure of 100080 Pa, while the air temperature at fan inlet was 5.4 °C. The speed of sound in such a medium reaches 334.5 m/s. Thus, the highest Mach number used in this case is 0.023. Therefore, as Mach number is significantly lower than 0.1, we selected "*Incompressible Ideal Gas*" model.

3 SIMULATION OF AN AIR DUCT USING CFD

3.1 Model of 3D air duct, fan and perforation

The simulations were executed based on 3D geometry modelled in Autodesk Inventor 2018 programme, which was further exported into ANSYS Workbench Release 19.1 systems. The overall ventilation system has 304 m, where the air duct is 300 m long. The air duct of 1 m diameter is composed of the discrete 30-metre ventilation pipes, between which 5-milimetre perforation is introduced to allow for partial air leakage into the surroundings. The size of perforations provides an average aperture of 0.0157 m^2 per each 30 m of the duct, or a square of 0.1253x0.1253 m. When an air duct is in operation, damage to the air duct occurs between the joints. However, to simplify the calculations, such damage was not introduced into the 3D model. At the start of the air duct there is a fan of 0.8 m diameter and length of 4 m, which complies with the technical specifications of Korfman AL8-55. In the model there are two measuring points with a distance of 210 m in between, in the form of planes in the air duct cross-section with a set boundary condition of "*interface*". These planes permit measurements of important quantities, such as pressure, air velocity, air temperature and gas density.

Vol. 68 (2022), No. 1
pp. 58–69, ISSN 1802-5420
DOI 10.35180/gse-2022-0069

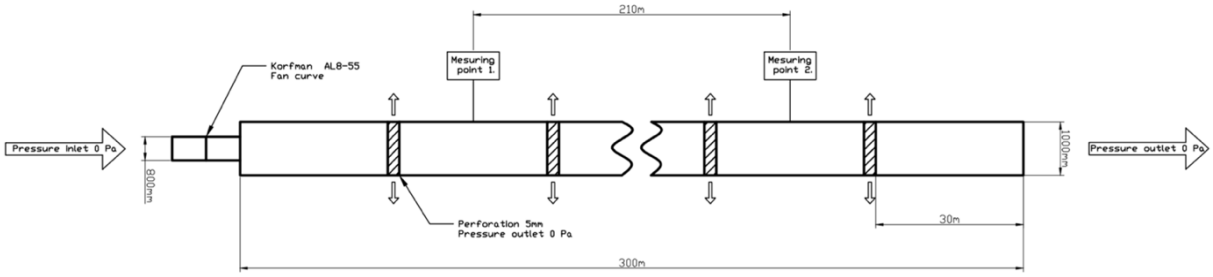

Figure 1. *Model of the 3D air duct system*

3.2 Boundary conditions

3.2.1 Fan sections

The modelled air duct is fitted with a fan Korfman AL8-55 of 0.8 m diameter. The engine output is 5500 W and the maximum total pressure is 630 Pa. At the air inlet, the boundary condition of "*Pressure Inlet*" is set for the turbulence intensity of 1 % and hydraulic diameter of 0.8 m. The air temperature at the inlet is 5.4 °C and the relative moisture is 61 %. In the site of axial vanes of the model cross-section, the boundary conditions of "Fan" is set, which puts the fan characteristics in operation. The fan is connected directly to the air duct and local resistance occurs in the site of a joint related to the fast expansion of the diameter. The operation characteristics were set based on the specifications provided by the producer website, i.e. Korfman. Thanks to the use of boundary conditions of "*Fan*", it is not necessary to simulate the whole complicated geometry of axial fan vanes, which simplifies the calculations and reduces the time needed to process the simulation [1]. To simulate the fan wall, we used the boundary condition "*Wall*", for which there is a zero "*Sand grain roughness*" due to the fact the linear resistance inside the machine was not the subject of research.

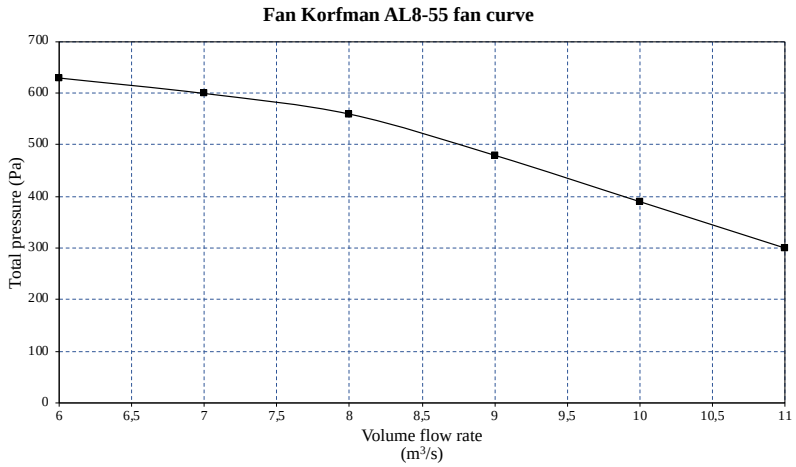

Figure 2. *Curve of the operation characteristic of Korfman AL8-55 fan*

3.2.2 Air duct section

The boundary condition of the air duct wall "*Wall*" determines the area of impermeable surface. As the term implies, it is a definition of a solid wall that delimits the flow between the fluid/ gas inlet and outlet. The set "*Sand Grain Roughness*" at the level of 0.0015 m in the test model of the ideally tight air duct ensured a specific aerodynamic resistance of 1-metre duct of 0.015 kg/m^8, which is a correct value according to [11], and best resembles the internal surface of the duct. Each square meter of the air duct surface is affected by thermal energy

Vol. 68 (2022), No. 1
pp. 58–69, ISSN 1802-5420
DOI 10.35180/gse-2022-0069

of 1 W, which causes slight heating of the air. Between the air duct pieces there are perforations to allow for air leaks. The perforations amount to 0.005 m between the two duct pipes. There is a set boundary condition "*Pressure outlet*" and pressure is 0 Pa, which means that there is no difference between the pressure at the wall and the ambient air. This boundary conditions are used to set the static pressure value. It is resistant to backflow, while it keeps a good solution convergence. In such a case, though, it is vital to determine other boundary conditions, such as temperature, or turbulent quantities. Due to the perpendicular air flow inside the air duct, the set values for "*Backflow Turbulent intensity*" and "*Backflow Turbulent Viscosity Ratio*" are high, 5 % and 10 respectively. The model is also affected by operation conditions, such as atmospheric pressure of 100080 Pa and ambient temperature of 5.4 °C.

3.3 Mesh – computing network

The network was created in the Ansys Meshing programme. The so-called "*Named Selections*" in the programme define the inlets, outlets and the wall. The network set-up largely influences the subsequent calculations, and thus it is important to select the maximum and minimum sizes of the elements correctly [12]. The maximum cell size is 0.25 m, minimum cell size 0.002 m, element shape is tetrahedrons and element smoothing is high.

The network comprises 567647 elements and 166181 nodes. The air duct walls have 5 layers of inflation of the first cell size of 0.008 m, the growth coefficient of the subsequent cells is 1.2 in order for the mean coefficient y+ to be 70. The network is denser at the fan, where the basic element size is 0.05 m. This allows for exact plotting of air pressure through the fan. Due to the low width of the perforation, i.e. 0.005 m, the network was denser there with the minimum cell size of 0.002 m near the perforation.

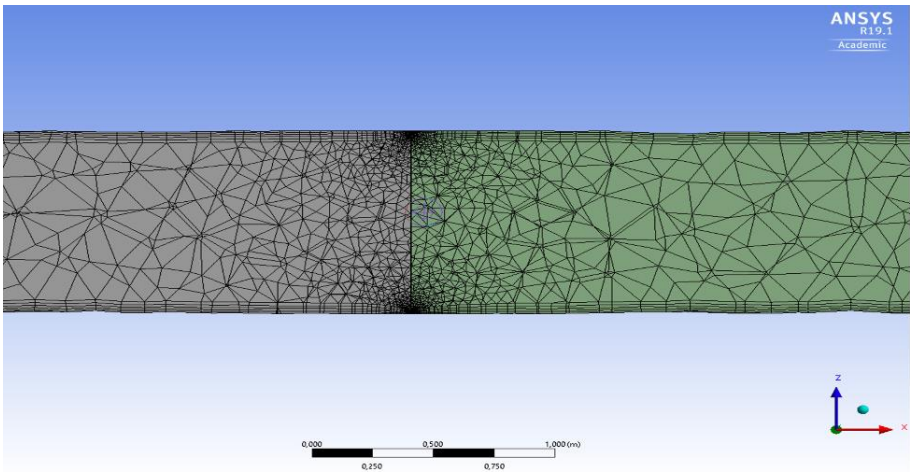

Figure 3. *Densification of the computing network in the vicinity of perforation – cross-section*

3.4 Mesh – quality assessment

MESH networks with sizes ranging from 500000 elements to 1600000 were produced. The study showed that network sizes above 570000 elements do not yield significant differences in computational results, so a number of elements oscillating around 560000 elements was considered optimal. To assess the network quality, the parameter Skewness was used, which is one of the primary measures of network quality. Skewness determines how close a cell shape is to ideal shape [13]. The ideal element is in case of value 0, while 1 means a completely degenerated element. This way, it is a ratio of the difference of the ideal cell size and the real cell size. For 3D flow, the value should be up to 0.4. In this model, the average skewness was 0.25, which corresponds to a low number of degenerated elements [14].

Vol. 68 (2022), No. 1
pp. 58–69, ISSN 1802-5420
DOI 10.35180/gse-2022-0069

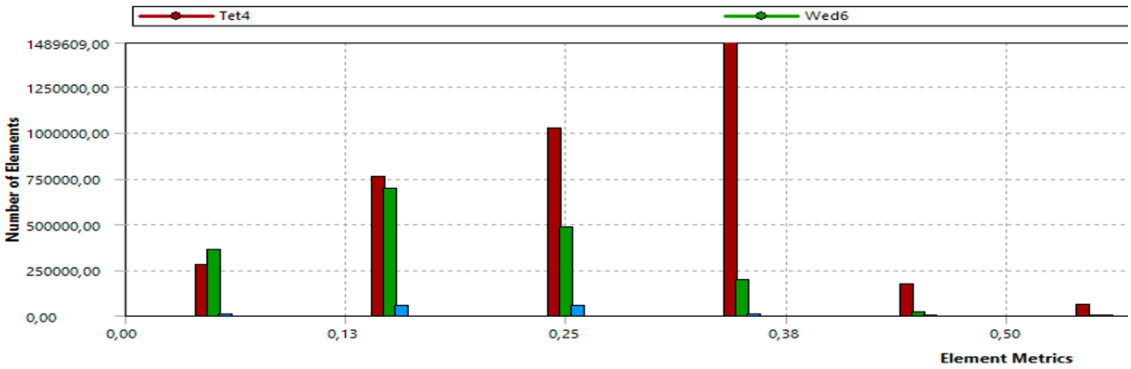

Figure 4. *Mesh quality assessment*

3.5 Simulation results

For each 1200 calculations, solution convergence was checked. The maximum difference of two corresponding quantities in the same point in two subsequent iterations (residuals) was reduced to 10^{-5}. An important part was also checking the modelling in the vicinity of the wall, where the standard wall function solution was used under the condition of turbulent flow [15]. There is a logarithmic formula for turbulent model k–ε, and its validity is limited by the value of dimensionless parameter y+> 40 ÷ 70. This condition was met. To evaluate the results, the important measuring points are located at the fan inlet, air duct outlet and two are inline. When measuring the real air duct parameters designed to ventilate mine workings and choosing the point measurement method of air velocity and its physical parameters, measurements are carried out at identical sites. The major physical parameters of air measured at the determined points are summarised in Table 2. Based on the data, it is possible to calculate all the coefficients to assess tightness, quality and energy efficiency of the air duct. Using the method described by [15], it is possible to calculate the aerodynamic specific resistance of 1-meter of air duct.

Table 1. *Results of modelling*

Fan inlet			**Air duct outlet**		
Static pressure	-143,74	(Pa)	Static pressure	0	(Pa)
Air speed	15,14	(m/s)	Air speed	7,61	(m/s)
Air density	1,25	(kg/m^3)	Air density	1,25	(kg/m^3)
Temperature	5,4	(°C)	Temperature	5,52	(°C)
Volume flow rate	7,61	(m^3/s)	Volume flow rate	5,98	(m^3/s)
Coordinate X	-4	(m)	Coordinate X	300	(m)
Pipeline dimension	0,8	(m)	Pipeline dimension	1	(m)
Measuring point 1.			**Measuring point 2.**		
Static pressure	255,16	(Pa)	Static pressure	39,93	(Pa)
Air speed	9,36	(m/s)	Air speed	7,72	(m/s)
Air density	1,25	(kg/m^3)	Air density	1,25	(kg/m^3)
Temperature	5,42	(°C)	Temperature	5,5	(°C)
Volume flow rate	7,35	(m^3/s)	Volume flow rate	6,06	(m^3/s)
Coordinate X	45	(m)	Coordinate X	255	(m)
Pipeline dimension	1	(m)	Pipeline dimension	1	(m)

Vol. 68 (2022), No. 1
pp. 58–69, ISSN 1802-5420
DOI 10.35180/gse-2022-0069

3.6 Fan work analysis

Ansys Fluent programme allows for an easy and fast modelling of gas flow transported under the influence of the pressure difference using the boundary condition "*Fan*". The chart below in Figure 5, plots the course of total pressure in the modelled fan axis. We can observe the maximum difference in the static pressure of 425.32 Pa, which together with dynamic pressure gives 569.06 Pa of difference of the total pressure between the fan inlet and outlets, under the air volume flow rate is 7.61 m^3/s. The difference in the total pressure calculated by CFD and the total pressure at the volume flow rate of 7.61 m^3/s is 4.76 Pa according to the producer's specifications. This result can be considered highly precise.

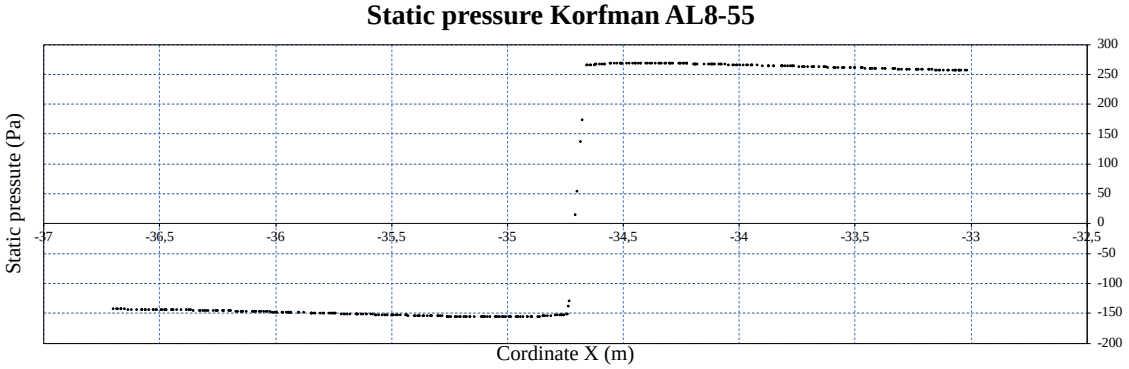

Figure 5. *Curve of fan static pressure*

3.7 Aerodynamic specific resistance of a 1-metre leaky air duct based on CFD model

The most important parameter describing the aerodynamic quality of air duct is the mass transfer coefficient – Θ $m^{2.5}/kg^{0.5}$ and the aerodynamic specific resistance of 1-metre air duct – r kg/m^8 [11]. The aerodynamic specific resistance of 1-metre air duct (r) predominantly depends on the used material, and even the air duct production technology. The total resistance of an ideally tight air duct is based on Atkinson's equation:

$$\Delta p = r \cdot L \cdot Q^2 \qquad \textbf{(6)}$$

where:

Δp – deduced pressure difference $[Pa]$,
r – aerodynamic specific resistance of 1 m section $[kg \cdot m^{-8}]$,
L – pipeline length $[m]$,
Q – air volume flow rate $\left[\frac{m^3}{s}\right]$.

The above-mentioned parameters in case of the designed air ducts are given in advance. If we investigate the aerodynamic quality of the existing systems, i.e. on the basis of measuring ventilation parameters, we determine the real aerodynamic specific resistance of 1-metre of air duct – r_e as follows [15]. First, we calculate the coefficient of the organic growth according to the formula:

$$a = \frac{1}{L} ln \left(\frac{V_w}{V_0}\right) \qquad \textbf{(7)}$$

where:

a – organic growth coefficient $[m^{-1}]$,
V_w – volume flow rate at the air duct outlet $\left[\frac{m^3}{s}\right]$,
V_0 – volume flow rate at the fan inlet $\left[\frac{m^3}{s}\right]$,

Vol. 68 (2022), No. 1
pp. 58–69, ISSN 1802-5420
DOI 10.35180/gse-2022-0069

L – air duct length $[m]$.

Next, it is important to calculate the real aerodynamic specific resistance of 1-metre of air duct according to the formula:

$$r_e = \frac{2a}{1-\exp(-2aL)}\left\{\frac{\Delta p_c}{V_0^2} - \frac{\rho}{2A^2}[\varsigma_w + \varepsilon + (\varsigma_0 - \varepsilon)\exp(-2aL)]\right\} \quad \textbf{(8)}$$

where:

Δp_c – fan total pressure [Pa],
ρ – air density $\left[\frac{kg}{m^3}\right]$,
A – surface area of the air duct cross-section $[m^2]$,
ε – type of auxiliary ventilation [suction :1; forced-air: -1],
ς_w – resistance coefficient at the air duct inlet [suction :1; forced-air: 0.6],
ς_0 – resistance coefficient at the air duct outlet [suction: 0.6; forced-air: 1],
r_e – real aerodynamic specific resistance of 1-metre of air duct $[kg \cdot m^{-8}]$.

The described flow of calculations is provided by, for example, the *Polish Central Mining Institute* (GiG) to assess the real air ducts functioning in the mine workings. For this reason, we used the method for our model. The result of the calculations is the coefficient of organic growth of $a = -8.035 \cdot 10^{-4}$ m^{-1}, and aerodynamic specific resistance of 1-metre of air duct of $r = 0.018029$ kg/m^8. Based on the investigation of 20 real air ducts in the operation of several mines [15], the aerodynamic specific resistance of 1-metre of unarmoured air duct of diameter 1 m ranges from 0.00822 to 0.01877 kg/m^8, where the mean value is 0.01406 kg/m^8. This means that the modelled air duct maintains the correct resistance corresponding to reality.

3.8 Investigation of the simulated air duct tightness

No air duct in the mine, in a driven tunnel or underground is absolutely tight [16], [2]. The size of the ventilation loss of leaky air ducts depends on the tightness of the different joints and the quality of air ducts (material wear and tightness), the length of the air duct, pressure difference inside and outside the air ducts, and the number and location of duct fans. The problems in making calculations for leaky air ducts in the mining business has been dealt with by a number of experts [17], [18], [13], as it is an important phenomenon but difficult to characterize using mathematical formulas. For these reasons, the model also included the factor of leakage.

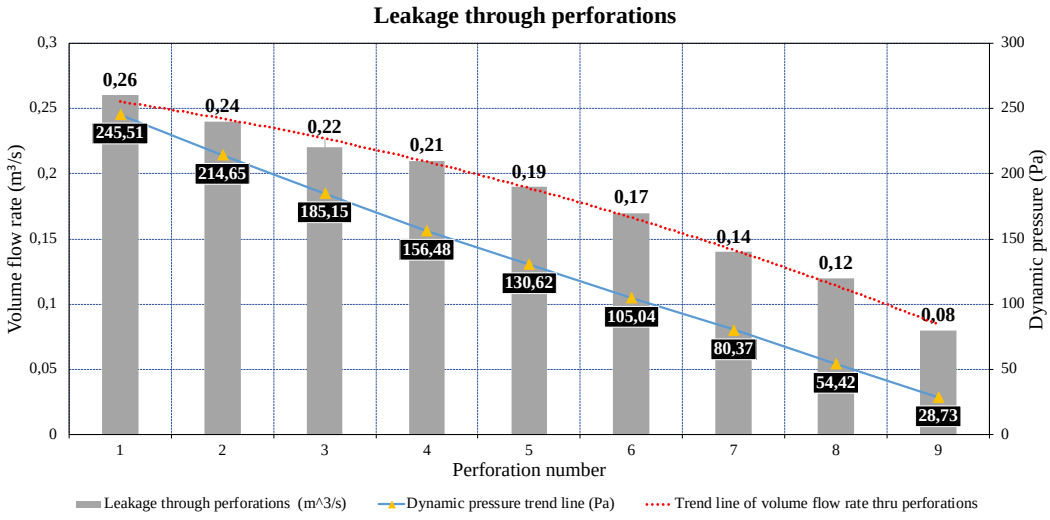

Figure 6. *Air leakage*

Vol. 68 (2022), No. 1
pp. 58–69, ISSN 1802-5420
DOI 10.35180/gse-2022-0069

Our research shows that the amount of air leakage depends on the total pressure inside the air duct. Air leakage decreases towards the air duct outlet because the relative total pressure is the lowest there [19]. We can also observe that the decrease in the quantity of leaked air is not linear against the static pressure drop. The air motion in the air duct is an example of flow with mass exchange with the medium. Research proved that the air quantity flowing through perforations is directly proportional to the square root of the difference in pressure in the air duct and in the mine workings. If we know the air duct resistance and its length, the leakage coefficient is determined as below [15]:

$$k = \sqrt{\frac{2\left(ln\frac{\frac{Q_W}{Q_O}}{0,77}\right)^3}{L^3}} \qquad \textbf{(9)}$$

where:

k – air duct leakage coefficient $\left[\frac{\mathrm{m}^3}{\mathrm{s}\cdot\sqrt{\mathrm{N}}}\right]$,
$\mathrm{Q_W}$ – flow rate at the fan inlet $\left[\frac{m^3}{s}\right]$,
Q_O – flow rate at the duct outlet $\left[\frac{m^3}{s}\right]$,
L – air duct length $[m]$.

Coefficient k characterizes the quality of the air duct tightness and means the following for the values $k \leq 1.5 \cdot 10^{-5}$ good impermeability, $1.5 \cdot 10^{-5} < k \leq 3 \cdot 10^{-3}$ sufficient impermeability, $k > 3 \cdot 10^{-3}$ insufficient impermeability. In case of the modelled air duct the coefficient k is $5.3 \cdot 10^{-4}$, which means that it is rather tight. Another method to assess the quality of air duct tightness is the mass exchange coefficient Θ $\mathrm{m^{2.5}/kg^{0.5}}$, which depends not only on the quality of fabric from which the duct is made, but mainly on the way how the duct is operated in the mine working. It is a method developed in *Polish Central Mining Institute* (GiG), and it is calculated as:

$$\Theta = 10^6 aA\sqrt{\frac{2a}{rA^2+2\varepsilon\rho a}} \qquad \textbf{(10)}$$

where:

Θ – mass exchange coefficient $\left[\frac{m^{2,5}}{kg^{0,5}}\right]$,
A – surface area of the air duct cross-section $[m^2]$,
ε – type of auxiliary ventilation [suction :1; forced-air: -1],
a – organic growth coefficient $[m^{-1}]$,
r – aerodynamic specific resistance of 1 m section $[kg \cdot m^{-8}]$,
ρ – air density $\left[\frac{kg}{m^3}\right]$.

Based on long-term research of *Polish Central Mining Institute* and [15], Table 2 gives the criteria to assess air duct tightness:

Table 2. *Evaluation of coefficient of mass exchange*

Coefficient of mass exchange Θ $\mathrm{m^{2.5}/kg^{0.5}}$	**Quality of air duct tightness**
$\Theta \leq 0.32$	Perfect (+5)
$0.32 < \Theta \leq 1.6$	Very good (5)
$1.6 < \Theta \leq 3.2$	Good (4)
$3.2 < \Theta \leq 16$	Almost good (-4)
$16 < \Theta \leq 21$	Rather good (+3)
$32 < \Theta \leq 160$	Satisfactory (3)

Vol. 68 (2022), No. 1
pp. 58–69, ISSN 1802-5420
DOI 10.35180/gse-2022-0069

$160 < \Theta \leq 320$	Bad (2)
$320 < \Theta \leq 1600$	Very bad (1)
$\Theta \geq 1600$	Fatal (0)

Therefore, to model an air duct the mass exchange coefficient Θ is 8.86 $m^{2.5}/kg^{0.5}$, which is based on the strict Knechtels criteria means that the ducts are almost well tight. To compare the results with reality, we carried a set of measurements using air duct fans used in driving several tunnels. The measurements were made using TESTO 440 device and the selected method was point measurements of air speed in air ducts and at the fan inlets. All the calculations were made on the basis of the equations stated in this paper, and the results are stated in Table 3.

Table 3. *Measurement results*

Place and date of measurements	Air duct diameter m	Air duct length m	Resistance of 1-metre sections kg/m^8	Mass exchange coefficient $m^{2.5}/kg^{0.5}$
Railway tunnel Milochov, Slovakia (10.08.2019)	2	639	0.000455943	0.32
Railway tunnel Milochov, Slovakia (17.12.2019)	2	989	0.000516736	168
Tunnel Prešov, Slovakia (20.10.2018)	1.6	140	0.001576952	0.12
Tunnel Prešov, Slovakia (20.10.2018)	1.6	220	0.001669714	0.14
Tunnel Mały Lubień Highway S7, Poland (14.03.2019)	2	885	0.000643567	29
Prague underground – section Pankrác – Depo Písnice, Czech Republic (07.06.2020)	0.6	120	0.15	0.46

The tables present results of experimental measurements carried out in a number of driven underground workings. Based on the results, we calculated the aerodynamic specific resistance of 1-metre section of air duct and the determined mass exchange coefficient approaches the CFD modelling results. The data show that, for the purposes of determining the required volume flow rates on the face, modelling a tight air duct may be conveniently complemented by a CFD model of leaky air duct, which renders more realistic results that are to be expected in practice.

4 CONCLUSION

Based on the evaluation of simulation results, we demonstrated that computational fluid dynamics successfully simulates all the phenomena occurring in an air duct, as well as for many tasks related to the ventilation of road tunnels and permits its precise design based on the modelling results. The analysis of air leakage showed the dependence of the distance of pressure source, which was Korfman AL8-55 fan in this case. The quantity of leaked air falls exponentially along with the length of the untight piping and depends on the static pressure. This confirms the correlation of the difference in air duct pressure and pressure in the mine workings and the air quantity flowing through the perforations. Therefore, the leakage coefficients Θ and k are largely affected by the apertures at the start of the air duct. This phenomenon was also reported by [5], where they proved the correlation of perforation location and the distance from the fan. Using the analytical procedure of the *Polish Central Mining Institute*, the calculated real resistance well corresponds with the real values stated by the producer. It was confirmed that using the function "*Sand Grain Roughness*" of 0.0015 m ensures the correct decrease in pressure. It further proved that the coefficients used to assess the existing air ducts are effective also in the CFD model.

Vol. 68 (2022), No. 1
pp. 58–69, ISSN 1802-5420
DOI 10.35180/gse-2022-0069

REFERENCES

[1] YI, H., J. PARK and M.S. KIM. Characteristics of mine ventilation air flow using both blowing and exhaust ducts at the mining face. *Journal of Mechanical Science and Technology*. 2020, vol. 34, pp. 1167–1174. ISSN 1738-494X. DOI: 10.1007/s12206-020-0218-0

[2] FRĄCZEK, R. *Aerologia górnicza: przykłady i zadania [Mining Aerology: Examples and Tasks]*. Gliwice: Politechnika Śląska, Katedra Elektryfikacji i Automatyzacji Górnictwa, 2010. ISBN: 83-915731-4-7.

[3] MOUJAES, S. and R. GUNDAVELLI. CFD simulation of leak in residential HVAC ducts. *Energy and Buildings*. 2012, vol. 54, pp. 534–539. ISSN 0378-7788. DOI: 10.1016/j.enbuild.2012.02.025

[4] TORAÑO, J., R. RODRÍGUEZ and I. DIEGO. Computational Fluid Dynamics (CFD) Use in the Simulation of the Death End Ventilation in Tunnels and Galleries. *WIT Transactions on Engineering Sciences*. 2006, vol. 52, pp. 113–121. ISSN 1743-3533. DOI: 10.2495/AFM06012

[5] AKHTAR, S., M. KUMRAL and A.P. SASMITO. Correlating variability of the leakage characteristics with the hydraulic performance of an auxiliary ventilation system. *Building and Environment*. 2017, vol. 121, pp. 200–214. ISSN 0360-1323. DOI: 10.1016/j.buildenv.2017.05.029

[6] TUTAK, M. and J. BRODNY. Analysis of the Impact of Auxiliary Ventilation Equipment on the Distribution and Concentration of Methane in the Tailgate. *Energies*. 2018, vol. 11(11), art. no. 3076. ISSN 1996-1073. DOI: 10.3390/en11113076

[7] KNECHTEL, J. Dobór instalacji lutniowej jako środek do zmniejszenia kosztów przewietrzania drążonych wyrobisk górniczych [Selection of air-duct ventilation system as a means to reduce ventilation costs of the driven workings]. *Przegląd Górniczy*. 2015, vol. 71(5), pp. 44–53. ISSN 0033-216X. Available at: http://yadda.icm.edu.pl/baztech/element/bwmeta1.element.baztech-80833871-4ec1-40fe-9e30-7052c3788931

[8] KNECHTEL, J. Wpływ jakości uszczelnienia lutniociągu elastycznego na koszty przewietrzania drążonego wyrobiska [The influence of air-tightness of a flexible air-duct on ventilation costs of the driven working]. *Przegląd Górniczy*. 2016, vol. 72(2), pp. 17–22. ISSN 0033-216X. Available at: http://yadda.icm.edu.pl/baztech/element/bwmeta1.element.baztech-369620e7-1490-4eb3-9075-0454b43e9caf

[9] OTÁHAL, A., J. MIČULEK and P. PROKOP. *Separátní větrání: příručka pro techniky důlního větrání [Auxiliary ventilation: a manual for mine ventilation technicians]*. Ostrava: VŠB – Technická univerzita Ostrava, Sdružení požárního a bezpečnostního inženýrství Ostrava, 1998. ISSN 80-86111-04-0.

[10] SULTANIAN, B. *Fluid Mechanics: An Intermediate Approach*. CRC Press, 2015. ISBN 9781466598980.

[11] WACŁAWIK, J. and W. ROSZCZYNIALSKI. *Aerologia górnicza [Mining Aerology]*. Warszawa: Państwowe Wydawnictwo Naukowe. 1989. ISBN 83-01-03876-4.

[12] KURNIA, J.C., A.P. SASMITO and A.S. MUJUMDAR. CFD simulation of methane dispersion and innovative methane management in underground mining faces. *Applied Mathematical Modelling*. 2014, vol. 38(14), pp. 3467–3484. ISSN 0307-904X. DOI: 10.1016/j.apm.2013.11.067

[13] BEŃACH, R. and D. PRAHL. *Computational Fluid Dynamics Analysis of Flexible Duct Junction Box Design*. U.S. Department of Energy, 2013. Available at: https://www.nrel.gov/docs/fy14osti/60710.pdf

[14] SASMITO, A.P., E. BIRGERSSON, H.C. LY and A.S. MUJUMDAR. Some approaches to improve ventilation system in underground coal mines environment – A computational fluid dynamic study. *Tunnelling and Underground Space Technology*. 2013, vol. 34, pp. 82–95. ISSN 0886-7798. DOI: 10.1016/j.tust.2012.09.006

[15] KNECHTEL, J. Jednostkowy opór aerodynamiczny lutniociągów zbudowanych z lutni elastycznych [Aerodynamic resistance of the air ducts made of flexible air pipes]. *Mechanizacja i Automatyzacja Górnictwa*. 2011, vol. 49(2), pp. 18–27. ISSN 0208-7448. Available at: http://yadda.icm.edu.pl/baztech/element/bwmeta1.element.baztech-article-AGHM-0035-0053

[16] WANG, Y.-Q., S. XU, R. REN, S. ZHANG and Z. REN. Application of the twin-tube complementary ventilation system in large-slopping road tunnels in China. *International Journal of Ventilation*. 2020, vol. 19(1), pp. 63–82. ISSN 1473-3315. DOI: 10.1080/14733315.2018.1549305

[17] TORAÑO, J., S. TORNO, M. MENÉNDEZ and M. GENT. Auxiliary ventilation in mining roadways driven with roadheaders: Validated CFD modelling of dust behaviour. *Tunnelling and Underground Space Technology*. 2011, vol. 26(1), pp. 201–210. ISSN 0886-7798. DOI: 10.1016/j.tust.2010.07.005

[18] GILLIES, A.D.S. and H.W. WU. Comparison of air leakage prediction techniques for auxiliary ventilation ducting systems. In: TIEN, J.C., ed. *Proceedings of the 8th US Mine Ventilation Symposium: June 11–17, 1999, Rolla, Missouri*. Rolla: Society for Mining, Metallurgy, and Exploration, 1999, pp. 681–690. ISBN 9781887009041. Available at: https://scholarsmine.mst.edu/cgi/viewcontent.cgi?article=1098&context=usmvs

[19] LIU, H., S. MAO and M. LI. A Case Study of an Optimized Intermittent Ventilation Strategy Based on CFD Modeling and the Concept of FCT. *Energies*. 2019, vol. 12(4), art. no. 721. ISSN 1996-1073. DOI: 10.3390/en12040721

[20] AI, Z.T. and C.M. MAK. Pressure Losses across Multiple Fittings in Ventilation Ducts. *The Scientific World Journal*. 2013, vol. 2013, art. no. 195763. ISSN 1537-744X. DOI: 10.1155/2013/195763